This article was downloaded by:
On: *22 January 2011*
Access details: *Access Details: Free Access*
Publisher *Taylor & Francis*
Informa Ltd Registered in England and Wales Registered Number: 1072954 Registered office: Mortimer House, 37-41 Mortimer Street, London W1T 3JH, UK

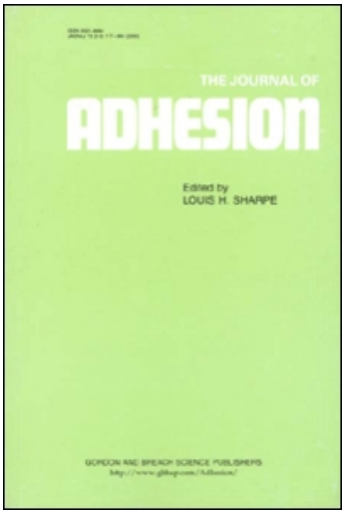

The Journal of Adhesion
Publication details, including instructions for authors and subscription information:
http://www.informaworld.com/smpp/title~content=t713453635

Structural Adhesive Bonds to Primers Electrodeposited on Steel

Robert T. Foister[a]; Richard K. Gray[ab]; Patricia A. Madsen[a]
[a] Polymers Department, General Motors Research Laboratories, Warren, Ml, U.S.A. [b] Buick-Oldsmobile-Cadillac Group, Warren, MI, U.S.A.

To cite this Article Foister, Robert T. , Gray, Richard K. and Madsen, Patricia A.(1987) 'Structural Adhesive Bonds to Primers Electrodeposited on Steel', The Journal of Adhesion, 24: 1, 17 — 46
To link to this Article: DOI: 10.1080/00218468708075414
URL: http://dx.doi.org/10.1080/00218468708075414

PLEASE SCROLL DOWN FOR ARTICLE

Full terms and conditions of use: http://www.informaworld.com/terms-and-conditions-of-access.pdf

This article may be used for research, teaching and private study purposes. Any substantial or systematic reproduction, re-distribution, re-selling, loan or sub-licensing, systematic supply or distribution in any form to anyone is expressly forbidden.

The publisher does not give any warranty express or implied or make any representation that the contents will be complete or accurate or up to date. The accuracy of any instructions, formulae and drug doses should be independently verified with primary sources. The publisher shall not be liable for any loss, actions, claims, proceedings, demand or costs or damages whatsoever or howsoever caused arising directly or indirectly in connection with or arising out of the use of this material.

J. Adhesion, 1987, Vol. 24, pp. 17–46
Photocopying permitted by license only
© 1987 Gordon and Breach Science Publishers, Inc.
Printed in the United Kingdom

Structural Adhesive Bonds to Primers Electrodeposited on Steel

ROBERT T. FOISTER, RICHARD K. GRAY† and PATRICIA A. MADSEN

Polymers Department, General Motors Research Laboratories, Warren, MI 48090-9055, U.S.A.

(Received October 11, 1986; in final form February 3, 1987)

Downloaded At: 15:38 22 January 2011

Adhesive bond strength and durability were investigated for steel substrates which had been cathodically electroprimed before bonding. Lap shear and torsional impact strengths of two model epoxy adhesives were evaluated. Very poor strengths and durability were found for one adhesive, which was cured with a mixture of three amine curing agents. Scanning electron microscopy and analysis of primer susceptibility to interaction with the curing agents suggested that, for the high concentrations of curing agent in the amine-cured adhesive, chemical and physical degradation of the primer occurred during cure at elevated temperature.

For the second adhesive, which was cured with a single imidazole catalyst, excellent strength and durability were obtained, with no evidence of primer degradation. Surprisingly, for this adhesive, strengths to primed steel were up to 88% higher than to cleaned (*i.e.*, degreased) bare steel. The concurrent improvements in environmental durability over bare steel, as assessed by water immersion and salt spray accelerated exposures, were attributed to the more favourable surface energetics of the adhesive/primer interface.

KEY WORDS structural adhesive; electrodeposited primer; epoxy adhesive lap shear strength; impact strength; moisture durability.

INTRODUCTION

Durable structural adhesive bonding of metallic automotive parts on a large volume scale awaits the solution of problems arising from

† Current Address: Buick-Oldsmobile-Cadillac Group, 30001 Van Dyke, Warren, MI 48090-9020, U.S.A.

surface contamination of the bonding substrates. In addition, however, even if cleaning procedures to remove oils, greases, drawing compounds and other processing lubricants were acceptable in the production environment, there is still an inherent weakness in the "clean" metal/adhesive bond. This weakness is due to the interface where a low surface energy organic material (adhesive) is mated to a high energy metallic oxide. Thus it has been repeatedly demonstrated[1,2] that even though initial strengths of metal-to-metal joints can be quite high, because of interface susceptibility to moisture degradation, such bonds invariably undergo some loss of strength in a moist environment. Moreover, degradation is accelerated if the joint is stressed during its service life.[3] Although joint design, choice of adhesive, and substrate pretreatment may be optimized to maintain an acceptable strength during service life, the inherent thermodynamic instability of the metallic oxide/adhesive interface in the presence of moisture remains.

Given this potential problem in bonding cleaned steel (or any other cleaned metal) with structural adhesives, together with numerous additional complications which arise in the displacement of surface contaminants from "uncleaned" substrates,[4] alternatives to bonding directly to cleaned *or* oiled steel substrates are clearly desirable. In an automotive production environment, all exterior metallic parts are primed for corrosion protection prior to painting. That is, the surfaces are first "phosphated", *i.e.*, a layer (0.6 μm) of zinc phosphate crystals is grown on the ferric oxide surface. An organic primer layer is then electro-deposited on top of the zinc phosphate. The thickness of this layer depends on process variables such as applied voltage, time, etc., but typically is 10 to 40 microns (see Figure 1). The surface formed in this manner is "ELPO-primed" where the term "ELPO" refers to the electrodeposition of the organic primer. This process provides a conversion coating by which a steel surface, initially unsuitable for painting, is rendered both paintable and corrosion resistant by offering to the paint a thermodynamically more compatible surface.[5] In principle, an ELPO-primed surface could perform a similar function in adhesive bonding, converting a high energy (therefore inherently unstable) steel/adhesive interface into a lower energy (therefore more stable) steel/phosphate/ELPO/adhesive interphase. Also, because adhe-

Downloaded At: 15:38 22 January 2011

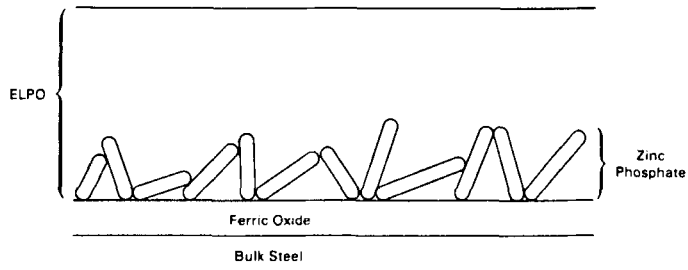

FIGURE 1 Schematic of electrodeposited primer/zinc phosphate/steel interphase.

sion between the primer and the corrosion-resistant phosphated steel is generally very good,[5] together with the fact that most adhesives will wet the primer upon application due to their similar surface energies, bonding to ELPO-primed steel could result in improved joint strength as well.

This work details a study of structural adhesive bonding to ELPO-primed steel surfaces. We address the following questions implicit in the foregoing discussion:

1) Can structural adhesives be used to bond ELPO-primed steel surfaces with strengths comparable to those achievable on cleaned steel?

2) Are bonds thus formed durable in a moist environment, and how do they compare with similar bonds to cleaned steel?

3) What difficulties may be encountered in this type of bond, and how can these difficulties be overcome?

In particular we consider in detail the environmental stability of adhesively bonded ELPO-primed steel joints from the point of view of surface energetics. A companion paper[6] discusses the strength of ELPO-primed steel joints *via* a finite element stress analysis.

EXPERIMENTAL

Materials

Two different unfilled epoxy adhesives, EA1 and EA2, were used in this work. The resins and curing agents (see Table I), with the

Downloaded At: 15:38 22 January 2011

TABLE I
Adhesive compositions

Material	Supplier	Description	phr†
EA1			
D.E.N. 431	Dow Chemical	Epoxy novolac resin	100
Epi-Rez 5048	Celanese	Tri-functional aliphatic epoxy resin	50
Versamide (V-25)	Dow Chemical	Polyamide curing agent	54
Epi-Cure 874	Celanese	Amine curing agent	4.5
Dicyandiamide	Eastman	Curing agent	1.5
EA2			
D.E.N. 431	Dow Chemical	Epoxy novolac resin	100
Epi-Rez 5048	Celanese	Tri-functional aliphatic epoxy resin	50
AP-V	Archem	1-(2-hydroxypropyl)-2-methylimidazole	9.5

† Parts per hundred resin with respect to D.E.N. 431.

Downloaded At: 15:38 22 January 2011

exception of the 1-[2-hydroxypropyl]-2-methylimidazole catalyst which was redistilled (145°C, 2 mm Hg) prior to use, were used as received. The adhesives were dispensed in precalibrated aliquots with a laboratory scale metering and mixing unit (Liquid Control Corporation, model CVR 2525).

Adhesive specimens

Mild steel lap shear (2.2 × 25.4 × 102 mm) and torsional impact shear (2.2 × 25.4 × 80 mm) coupons were phosphated (Chemfil process #168), then cathodically electro-primed prior to bonding. Most of the samples in this investigation received a Uniprime 3043 (PPG Industries) treatment. However, in the latter stages of this work, we also investigated the properties of Uniprime 3150A. The samples were primed under the following conditions:

ELPO Tank Temperature—30°C
Application Voltage —250 V
Time —2 min.

The two primers differ primarily in their recommended cure schedule. For Uniprime 3043, samples were cured for 0.5 h at 177°C, while for Uniprime 3150A, the samples were cured for 0.5 h at 160°C. Resultant primer thickness was approximately 0.025 mm.

Cleaned mild steel coupons for lap shear and torsional impact samples were prepared by first vapor-degreasing with 1,1,1-trichloroethane, followed by vapor blasting with Novacite 200 in water at 500 kPa. Standard (ASTM D1002) samples were then prepared from the ELPO-primed and cleaned steel coupons, with a bond overlap of 12.7 mm and a bond thickness of 0.127 mm. Following adhesive cure (for details, see below), lap shear samples were tested on an Instron (Model TTC) testing machine using a crosshead speed of 1.27 mm/min. Lap shear strength was determined from the maximum load reached prior to, or at bond rupture. Torsional impact shear samples were tested on a Tinius Olsen impact test machine with a pendulum impact velocity of 0.33 m/sec. All lap shear tests were carried out at room temperature. In addition to tests at room temperature, torsional impact testing was also carried out at −20°C, 25°C, 60°C, and 125°C by equilibrating the test samples in an environmental chamber.

Downloaded At: 15:38 22 January 2011

Specimens for surface energy analysis

Flat sheets of EA1 and EA2 were free cast on sheets of Teflon, and subjected to the oven cure described below. Contact angles on the EA1 and EA2 surfaces using the various well-characterized liquids described in Table II were measured with the Kernco Model G-II Contact Angle Goniometer. Specific procedures for determining surface energies, interfacial energies, and bond stability are outlined in the Appendix.

TABLE II
Total (γ_{LV}), polar (γ^p_{LV}), and dispersive (γ^d_{LV}) surface energies of various liquids

	γ_{LV} (mJm^{-2})	γ^p_{LV} (mJm^{-2})	γ^d_{LV} (mJm^{-2})	$\gamma^p_{LV}/\gamma^d_{LV}$
Water†	72.2	50.2	22.0	2.3
Glycerol†	64.0	30.0	34.0	0.88
Formamide†	58.3	26.0	32.3	0.80
Diiodomethane†	50.8	2.3	48.5	0.05
Ethylene glycol‡	48.3	19.0	29.3	0.65
1-bromonaphthalene†	44.6	0.0	44.6	0.00
Tricresylphosphate†	40.9	1.7	39.2	0.04

† Ref. 10.
‡ Ref. 7.

Initial adhesive cure

Each adhesive was cured by two different methods. "Oven cure" consisted of initially subjecting the samples to a 150°C forced air oven for twenty-five minutes. For oven cure, all samples were held in a fixture designed to give 100 kPa clamping pressure, and the fixture was heated before sample assembly. The second method of cure involved rapid inductive heating of the steel coupons using electromagnetic energy (100 kHz, 5 kW) supplied by a Pulsonix Magnetic Thermal Generator (Dimensional Research Corporation Model PI 5000-A). Energy dissipated by the induced current heats the surface of the specimen in contact with the adhesive, thereby initiating rapid cure (see Figure 2). Surface temperature measurements indicated that the maximum surface temperature generated under the present conditions (2.5 sec, 100% power) was approximately 180°–200°C. This method provided excellent initial strength for the samples prior to the thermal cycling (post cure) described below.

Downloaded At: 15:38 22 January 2011

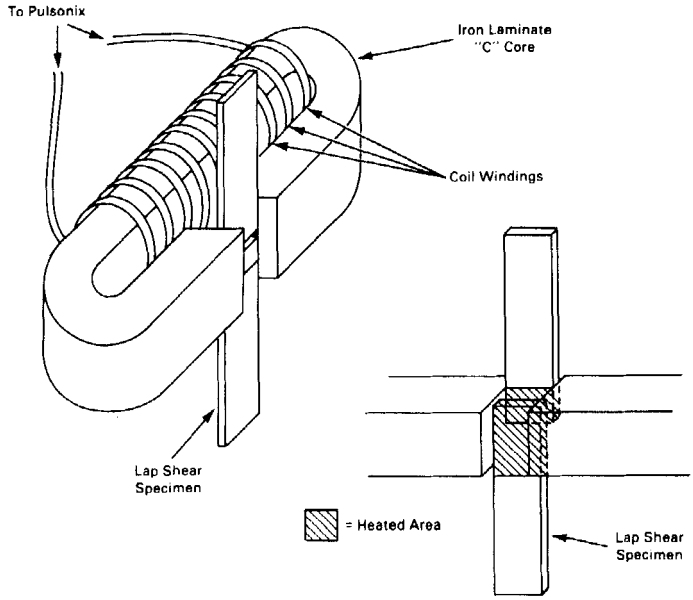

FIGURE 2 Induction heating coil used in preparation of lap shear samples.

Post-cure cycle

All samples (except those tested immediately and after room temperature exposure) were post-cured prior to environmental exposure. Post-cure consisted of the following cycle which simulates a typical automotive paint-bake process:

1) 75 minutes at 160°C
2) Cold tap water quench
3) 30 minutes at 135°C
4) Room temperature cooling for 45 minutes
5) 20 minutes at 135°C
6) Room temperature cooling for 45 minutes
7) 40 minutes at 160°C

Downloaded At: 15:38 22 January 2011

Environmental exposures

Effects of environmental exposure were assessed with reference to controls, for a seven-day, 60°C water immersion, and for an eight-week (5% NaCl at 38°C) salt spray environment. Controls were tested after comparable exposure times at room temperature. Both water immersion and salt spray samples were tested within two hours after removal from environment.

Samples for assessment of primer degradation

In addition to the Uniprime ELPO primers (3043, 3150A) used in adhesive sample preparation, six additional cathodic electrodeposition primers were assessed for primer degradation at elevated temperatures. These included PPG products ED 3002V, ED 3048, ED 3050, and ED 3250. Primers I045 and I059 from Inmont Corporation were also tested. The samples were prepared using regular mild steel paint panels, and the Chemfil 168 zinc phosphating treatment "Normal" cure ("N" designations) of the primers refers to the supplier recommended cure, while "undercured" and "overcured" ("U" and "O" designations, respectively) refer to 0.25 h, 20°C less and 0.25 h, 20°C more than the normal cure time and temperature.

Thermal stability measurements

Thermal stability of the 3150A primer was monitored using thermogravimetric analysis (TGA). The test apparatus consisted of a DuPont 990 Thermal Analyzer coupled with a DuPont 943 TGA module and Omnitherm Data System. A sample of cured primer, weighing approximately 5 mg, was scanned in the TGA module from 25–600°C in a nitrogen atmosphere, and from 600–850°C in an air atmosphere both at a rate of 20°C/min. Data was recorded as weight loss *versus* temperature. Pyrolyzates from the TGA scan were also collected and analyzed by infrared spectroscopy (IR).

Scanning electron microscopy

Lap shear failure surfaces were examined with a scanning electron microscope (ISI Industries), in conjunction with an attached energy dispersive analyzer.

Downloaded At: 15:38 22 January 2011

RESULTS AND DISCUSSION

EA1 on Uniprime 3043

Our initial attempt to bond steel electrodeposited with Uniprime 3043 with the EA1 adhesive was unsuccessful. With the exception of the room temperature cure (216 h), both lap shear and torsional impact specimens showed very low initial and control strengths, as well as extensive strength loss in water soak and salt spray environments. The data are given in Table III (lap shear) and Table IV (torsional impact). Visual inspection of the failure surfaces revealed a mixed failure mode in the phosphate/ELPO/adhesive interphase region. In addition, almost all surfaces exhibited extensive blistering and degradation of the ELPO primer layer. There were no readily apparent qualitative differences in ELPO degradation between induction and oven-cured specimens. Likewise, there were no significant differences in strength or strength retention for samples cured by the two methods.

TABLE III
Lap shear strengths (kPa): EA1 and EA2 on uniprime 3043 substrates

Adhesive	Cure	Environment	Strength
EA1	Oven/post-cure	Control	4,800 890
	Oven/post-cure	Water immersion	2,300 2200
	Oven/post-cure	Salt spray	1,200 320
	Induction	Immediate test	9,500 1500
	Induction/post-cure	Control	4,400 250
	Induction/post-cure	Water Immersion	2,400 770
	Induction/post-cure	Salt spray	1,900 750
	Room temperature (216 h)	Immediate test	12,200 610
EA2	Oven/post-cure	Control	29,000 1300
	Oven/post-cure	Water immersion	27,600 680
	Oven/post-cure	Salt spray	29,700 1600
	Induction	Immediate test	16,000 2000
	Induction/post-cure	Control	29,100 1300
	Induction/post-cure	Water Immersion	27,200 2500
	Induction/post-cure	Salt Spray	27,400 2100
	Room temperature (216 h)	Immediate test	27,500 1200

TABLE IV
Room temperature torsional impact strengths (kJm^{-2}): EA1 and EA2 on uniprime 3043 substrates

Adhesive	Cure	Environment	Strength
EA1	Oven/post-cure	Control	—†
	Oven/post-cure	Water immersion	—†
	Oven/post-cure	Salt spray	—†
	Induction	Immediate test	5.16 1.1
	Induction/post-cure	Control	2.30 1.4
	Induction/post-cure	Water Immersion	2.70 1.4
	Induction/post-cure	Salt spray	3.16 2.2
	Room temperature (216 h)	Immediate test	10.6 2.8
EA2	Oven/post-cure	Control	17.8 3.5
	Oven/post-cure	Water immersion	19.6 5.5
	Oven/post-cure	Salt spray	14.7 5.0
	Induction	Immediate test	7.18 1.3
	Induction/post-cure	Control	23.3 3.5
	Induction/post-cure	Water Immersion	27.6 2.3
	Induction/post-cure	Salt spray	20.5 6.7
	Room temperature (216 h)	Immediate test	21.1 5.2

† Highly variable, inconsistent data.

Downloaded At: 15:38 22 January 2011

SEM's of EA1/Uniprime 3043 failure surfaces

As indicated above, failure surfaces of the EA1/Uniprime 3043 system showed blistering and general degradation of the ELPO primer. An example of this degradation on matching surfaces of an induction cured lap shear specimen after seven-day, 60°C water immersion is shown in Figure 3. Note especially the cellular, foam-like structure. Higher magnification (Figure 3C) shows that these cells often contain a central region of exposed phosphate crystals. This indicates that the underlying phosphate layer was exposed by a physical or chemical "etching" action during bond formation, rather than upon fracture.

The cell-like structure was not confined to water-soak specimens, nor just to lap shear specimens, as matching surfaces of an immediate test, impact specimen show (Figure 4A, B). Close inspection revealed that one surface (Figure 4A) showed no phosphate exposed in the cells, while in the matching surface (Figure 4B) many cells showed a faint white center. Upon higher magnification, it was apparent that this center was similar to the region shown in Figure 3C. Foaming or etching (which creates the cells) apparently was localized within the primer region, rather than in the adhesive, as shown schematically in Figure 4C. This zone of degradation generally resulted in a weak "interphase" which has a potential for stress concentration, as well as for accelerating the accumulation of moisture in the bond (by "wicking," for example).[1]

As shown in Figures 5A, shear testing appeared to tear the cells, while impact testing (Figure 5B) apparently fractured the cells in a smooth, slicing action. Figure 5A, B illustrates clearly the differences in shear *versus* impact loading of the specimens.

Finally, in the samples which underwent salt spray exposure, there were numerous planar cystals of NaCl* dispersed among the cells structures. Figure 6 shows one such crystal on the surface of an oven cured, impact specimen failure surface. Thus, it is likely that these crystals grew during bond exposure *via* wicking of salt solution. Consequently, in salt spray, as in ambient (control) and water immersion environments, the degraded EPLO primer layer obviously contributed to poor bond strength and durability.

* As determined by energy dispersive spectroscopy.

Downloaded At: 15:38 22 January 2011

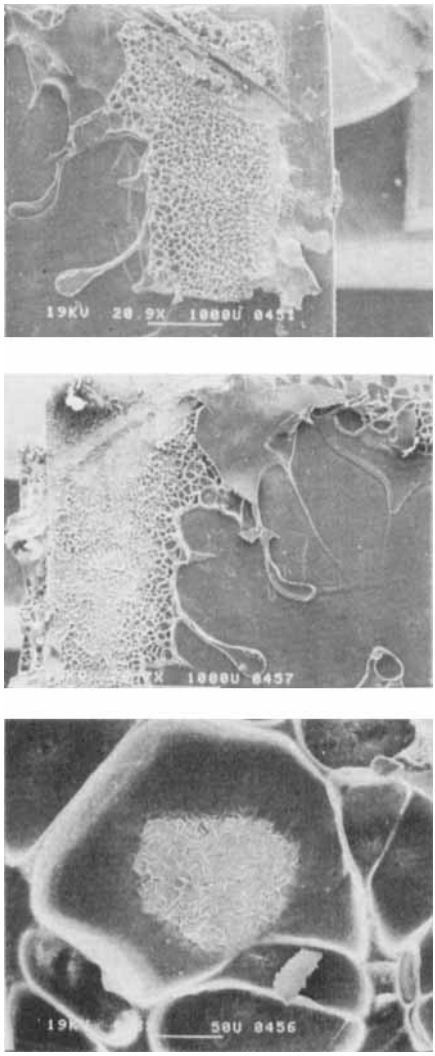

FIGURE 3 Scanning electron microscopy of EA1/Uniprime 3043 failure surfaces. (a) seven day, 60°C H_2O (lap shear), (b) matching surface of (a), (c) degradation cell (note exposed phosphate crystals).

Downloaded At: 15:38 22 January 2011

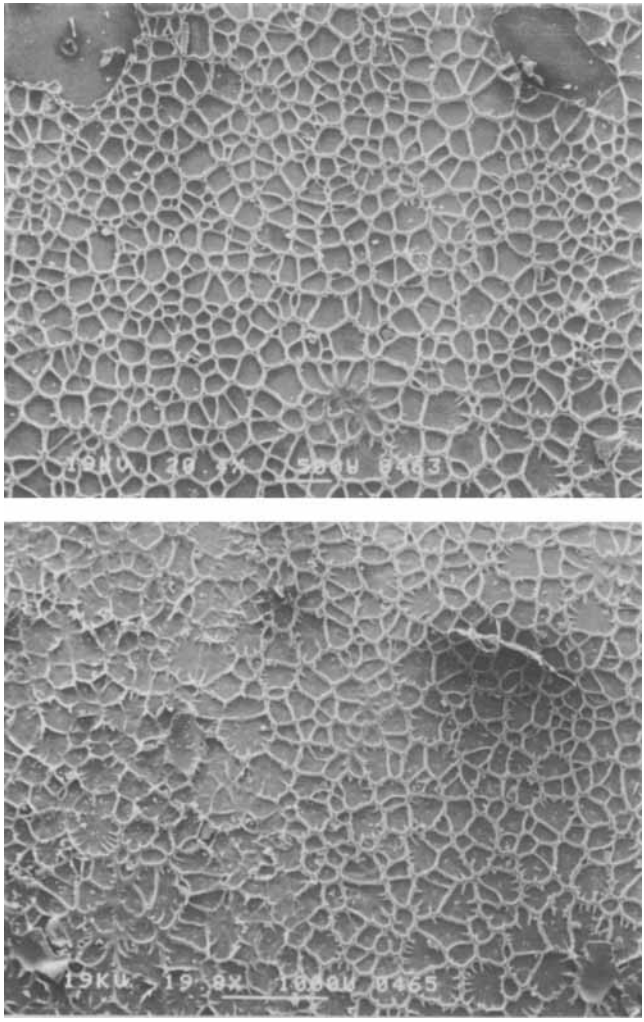

FIGURE 4 (a) EA1/Uniprime 3043 failure surface–room temperature cure (torsional impact), (b) matching surface of (a). (c) schematic of fracture path through degradation cell.

Downloaded At: 15:38 22 January 2011

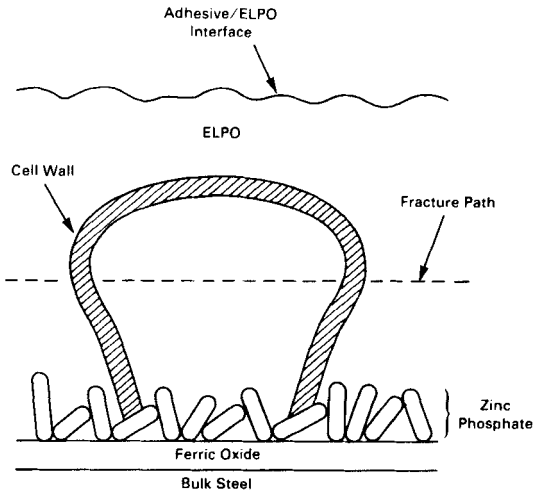

FIGURE 4 (*Continued*)

Downloaded At: 15:38 22 January 2011

General aspects of primer degradation

Interaction with the Adhesive Given evidence of primer degradation, we first investigated the possibility that certain component(s) of the adhesive caused the problem. Assuming that one (or all) of the curing agents in EA1 was responsible, we placed drops of the curing agents on an ELPO-primed steel coupon. The specimens were then heated in an oven at 100°C for five minutes. All of the curing agents gave the appearance of solubilizing the primer, as evidenced by dissolution of the primer accompanied by foaming. Furthermore, light scraping of the exposed area of the coupon with a wooden stick completely displaced the EPLO layer, leaving what appeared to be a bare metal surface. It, therefore, appeared that the curing agents were likely contributors to the degradation observed on the various failure surfaces. However, when pure resin and diluent were tested in a similar manner, they also weakened the primer, so that again light scraping with a wooden stick exposed bare metal. However, in contrast to the curing agents, no evidence of foaming was seen.

Next we tested a number of different primer systems, with a variety of curing agents, resins, diluents, and high boiling liquids.

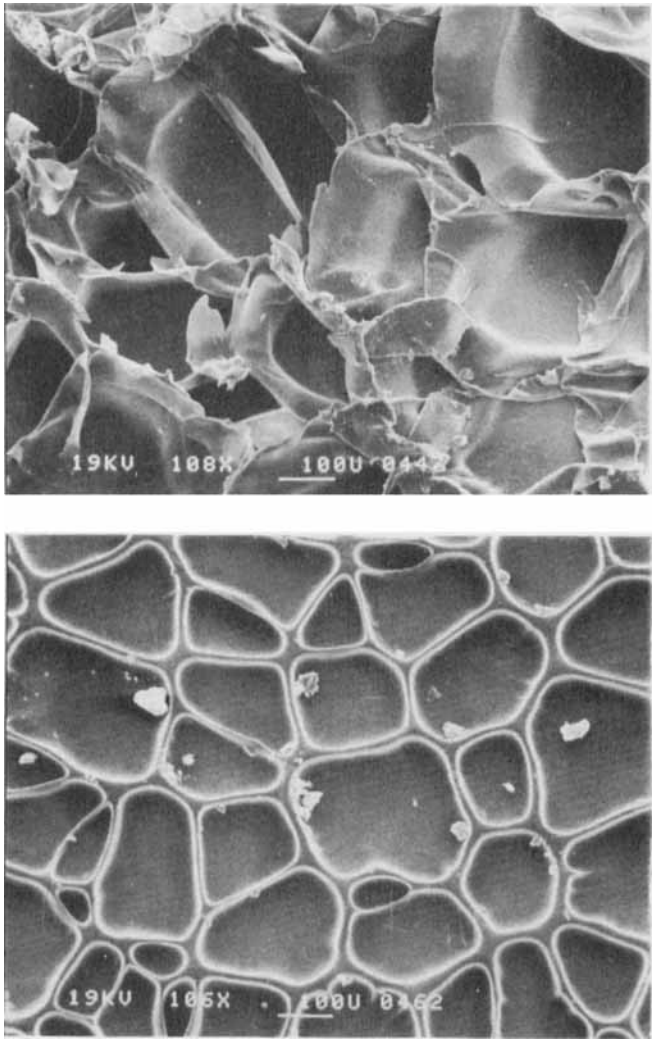

A)

B)

FIGURE 5 EA1/Uniprime 3043 failure surfaces: (a) seven day, 60°C H_2O (lap shear), (b) seven day, 60°C H_2O (torsional impact).

Downloaded At: 15:38 22 January 2011

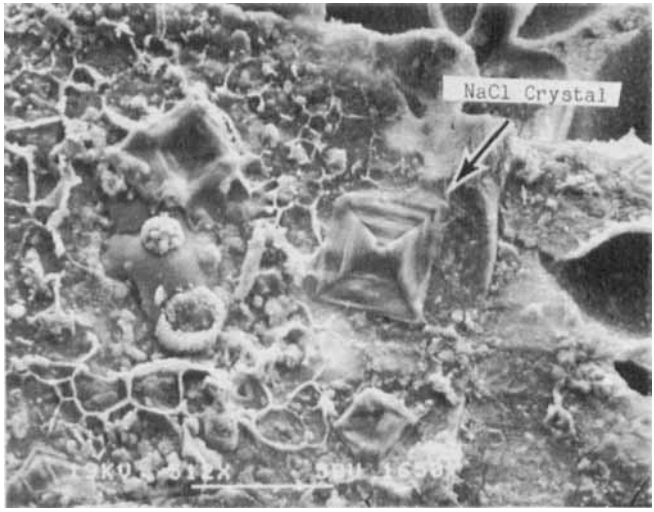

FIGURE 6 EA1/Uniprime 3043 failure surface: eight week salt spray (torsional impact).

As shown in Table V, the phenomenon of chemical and physical degradation of primers was not confined to the system we had used in the adhesion studies. In fact degradation was the rule, rather than the exception. With reference to Table V, degradation occurred at a temperature as low as 67°C for a primary amine(diethylenetriamine) on underbaked Uniprime 3250, or as high as 141°C for the epoxy novolac resin on the 3002 primer.

An important general implication of the work just described is that ELPO degradation need not occur solely with a structural adhesive bonding process. Any material brought into contact with the primed surface at an elevated temperature is a potential source of problems stemming from primer degradation. In the case of the EA1 adhesive, we evidently had an example of one of the more harmful mainfestations of primer degradation.

Loss of Volatiles from the Primer Another possible source of primer degradation during adhesive cure, or during elevated temperature post cure, is loss of volatile components from the primer. We would expect this to be particularly likely were the primer not sufficiently cured prior to bonding. Two primers, Uniprime 3150A

Downloaded At: 15:38 22 January 2011

TABLE V
Primer degradation temperatures (°C)
Primer (N = normal bake, U = underbaked, O = overbaked)

Liquid	3043 (N)	3002V (U)	3002V (O)	3002V (N)	3048 (N)	3050 (U)
Resin A	120	109	124	141	119	126
Resin B	116	125	128	140	125	125
Diluent A	120	126	127	134	125	121
Curing agent A	119	124	122	124	122	124
Diluent B	74	83	80	75	77	70
Curing agent B†	71	74	75	75	68	75
Catalyst	94	108	112	114	111	114
Mineral oil	154	—	—	—	—	—
Glycerol	165	—	—	—	—	—

† Obvious chemical reaction on all primers.

Primers
3002 V—Cathodic ELPO (PPG)
ED 3043—Uniprime Cathodic ELPO (PPG)
3048—Uniprime Cathodic ELPO (PPG)
3050—Uniprime Cathodic ELPO (PPG)
3150—Uniprime Cathodic EPLO (PPG)
3250—Uniprime Cathodic ELPO (PPG)
I045—Cathodic ELPO (Inmont)
I059—Cathodic ELPO (Inmont)

Downloaded At: 15:38 22 January 2011

and 3043, were therefore subjected to thermogravimetric analysis (TGA). These two primers differ primarily in their cure schedule, with the Uniprime 3150A baked at 160°C for 0.5 h, and 3043 at 177°C for 0.5 h.

The area of interest is the room temperature to 200°C section of the TGA scan, as this is the temperature range generally encountered in adhesive cure and post cure cycles. In this range weight loss due to evolution of volatiles was first observed at a temperature as low as 190°C. These volatiles are believed to be due to thermal degradation of the primer or are, perhaps, by-products of further curing.

Attempts were made using IR to identify the volatiles liberated during the thermal stability measurements by analyzing the pyrolyzates collected from the TGA scan (up to 600°C). The IR spectra obtained were attributed to bisphenol A, to an ester, and to an unidentified component with a main band at 1620 cm^{-1}. The exact chemical composition of Uniprime 3150A is proprietary, so no

TABLE V (Continued)

3050 (N)	3050 (O)	3150 (U)	3150 (O)	3250 (U)	3250 (N)	I045 (N)	I059 (N)
126	130	122	133	124	126	131	129
122	124	126	136	126	125	128	126
123	125	123	126	123	123	123	119
124	125	119	123	122	116	124	120
75	75	74	73	70	72	73	70
72	71	70	74	67	72	75	73
115	114	109	109	109	112	112	112
—	—	—	—	—	—	—	—
—	—	—	—	—	—	—	—

Liquids
Resin A—D. E. N. 431 (epoxy novolac)
Resin B—Epon 825 (diglycidylether of bisphenol A epoxy) (Shell)
Diluent A—Epi-Rez 5048 (aliphatic trifunctional epoxy) (Celanese, Inc.)
Diluent B—Phenylglycidylether (Aldrich)
Curing Agent A—Versamide V-25, polyamide curing agent (Dow)
Curing Agent B—Diethylene triamine (Aldrich)
Catalyst—AP-V (1-(2-hydroxypropyl)-2-methylimidazole)

Downloaded At: 15:38 22 January 2011

definite conclusions as to the source of the volatiles were possible. For Uniprime 3043 the TGA and IR results were very similar to those for 3150A.

Thus, in both cases, volatile loss from the primers first occurred at temperatures within the range of adhesive processing parameters (~190°C). These results suggest that volatiles liberated at elevated temperatures could also be in part responsible for the observed foaming and loss of adhesive bond integrity. This is in addition to chemical attack of the primer by various components of typical epoxy adhesives.

EA2 on Uniprime 3043

Although, according to Table V, the degradation temperature varied somewhat with the chemical nature of the curing agent, there was no reason *a priori* to expect that imidazoles, as opposed to

TABLE VI
Lap shear strengths (kPa): EA2 on cleaned steel substrates

Cure	Environment	Strength
Oven/post-cure	Control	20,600 ± 2,100
Oven/post-cure	Water immersion	18,700 ± 1,300
Oven/post-cure	Salt spray	15,200 ± 1,200
Induction	Immediate test	24,700 ± 1,900

stoichiometric curing agents (*e.g.*, primary amines), would eliminate primer degradation. On the other hand, taking into account that high levels of the amine curing agents, together with elevated temperatures during cure, were apparently partially responsible for the primer degradation observed with EA1,* for our second attempt to bond to Uniprime 3043, we reformulated the adhesive by substituting a single imidazole catalyst, 1-(2-hydroxypropyl)-2-methylimidazole, at a much smaller concentration. For this adhesive (EA2) the resin and diluent were unchanged.

In marked contrast to EA1, Tables III and IV show very high initial and control strengths for EA2, as well as excellent strength retention for both water immersion and salt spray exposures. For ELPO-primed substrates, initial and control strengths were up to 88% higher than those obtained with the same adhesive, on degreased steel (Table VI). In addition, from the data given in Tables III and VI, it can be shown that lap shear strength retention for EA2 on Uniprime 3043 was higher for water immersion (~95% compared to ~91%) and for salt spray exposure (~100% compared to ~75%), than for the same adhesive on degreased steel subjected to these same accelerated exposures.

We also investigated the variation in torsional impact strength with temperature, comparing cleaned steel substrates to substrates primed with Uniprime 3150A. As shown in Figure 7 (see also Table VII), over the range of test temperatures (−25°C to 125°C), bonds to ELPO-primed substrates were stronger in torsional shear than bonds to cleaned steel. At room temperature and at 60°C, in fact,

* According to additional (unpublished) work in this laboratory, commercially available adhesives utilizing high levels of amines have also shown poor performance attributable to primer *degradation*.

Downloaded At: 15:38 22 January 2011

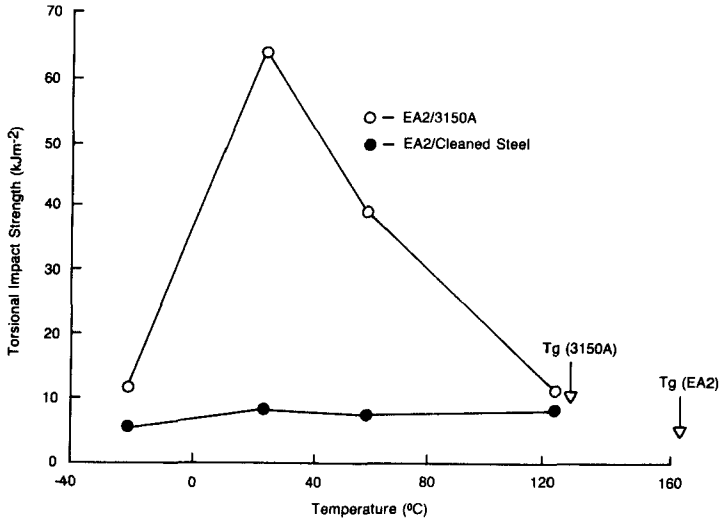

FIGURE 7 Variation of torsional impact strength with temperature for EA2.

bonds to primed substrates gave dramatic increases in strength. At the lowest and highest temperatures, improvements in strength were less dramatic. The fact that the data for EA2 on cleaned steel showed no significant variation over the temperature range of −25°C to 125°C is related to the fact that all of these temperatures are less than the glass transition temperature (167°C) of EA2.

For Uniprime 3150A, on the other hand, the glass transition temperature (128°C) was very close to the highest test temperature (125°C). Since failure was located in the primer, and since the primer would likely undergo considerable loss in modulus and strength in this temperature range, it is not surprising that the higher strengths at 25°C and 60°C would decrease to the lower value at 125°C.

TABLE VII
Torsional impact strength (kJm^{-2}) as a function of temperature

Adhesive/Substrate	Temperature (°C) −20	25	60	125
EA2/Cleaned steel	6.31 ± 7.0	8.06 ± 2.1	7.36 ± 1.1	8.06 ± 7.0
EA2/3150A	12.2 ± 4.5	64.7 ± 8.7	39.1 ± 4.4	12.2 ± 4.3

Downloaded At: 15:38 22 January 2011

In general then, there was a very dramatic increase in strength (both lap shear and torsional impact) as well as a substantial increase in durability for bonds to ELPO-primed, as opposed to cleaned steel substrates.

SEM's of EA2/uniprime 3043 failure surfaces

In contrast to the EA1/Uniprime 3043 failure surfaces, which showed blistering, cell structure, and general degradation of the primer, no obvious signs of degradation were apparent on any of the EA2/Uniprime 3043 surfaces examined. In all cases, except where the failure mode was mixed (phosphate/primer/adhesive and cohesional within the adhesive itself), the failure mode was solely within the phosphate/primer region. Figure 8A shows a mixed phosphate/primer failure surface occurring at the edge (a high stress area in the lap shear test) of an "immediate test" specimen which had been induction cured, but which had not been subjected to post-cure. The remaining areas of the matching fracture surfaces for this case were characterized by large amounts of adhesive on both sides, indicating cohesive failure of the adhesive. With this exception, all other test and cure conditions yielded failures which were qualitatively similar: no cohesional failure of the fully cured adhesive, but failure within the phosphate/primer region. Representative SEMs of these failure surfaces are shown in Figure 8B (oven cure control, impact) and Figure 8C (room temperature cure, lap shear). On none of the samples did the SEM's reveal any evidence of primer degradation. We can, therefore, conclude that by reformulating the adhesive to reduce the high concentration of curing agent present in EA1, the major source of primer degradation had been eliminated. However, since this result has generally been shown to be quite specific to imidazole-type catalysts, and is the basis of a patented adhesive system for bonding to primed steel,[15] the chemical nature of the curing agent is undoubtedly a factor. Loss of volatiles during post-cure did not appear to play a role in these systems.

Surface energy and stability analysis of primer/adhesive and steel/adhesive bonds

The increases in strength observed for bonds to primed, as opposed to cleaned, steel are attributable to differences in the way stress is

Downloaded At: 15:38 22 January 2011

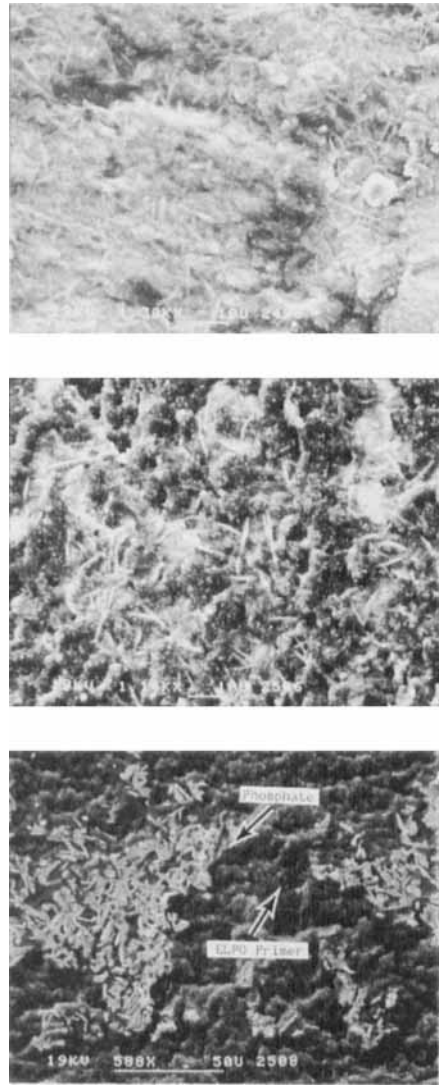

FIGURE 8 EA2/Uniprime 3043 failure surfaces: (a) immediate test (lap shear) (b) control (torsional impact) (c) seven day, 60°C H_2O (lap shear).

Downloaded At: 15:38 22 January 2011

Downloaded At: 15:38 22 January 2011

TABLE VIII
Average† equilibrium advancing contact angles (θ_e) and standard deviations (σ)

Liquid	432/5048 (EA1) θ_e	432/5048 (EA1) σ	431/5048 (EA2) θ_e	431/5048 (EA2) σ	Uniprime 3043 θ_e	Uniprime 3043 σ	Degreased 1020 Steel θ_e	Degreased 1020 Steel σ
Water‡	71.4	4.8	86.9	6.8	72.8	3.9	41.4	3.7
Glycerol	65.8	2.6	73.9	3.9	66.0	2.9	36.9	5.6
Formamide	56.2	4.5	66.5	7.5	61.0	2.6	31.0	7.1
Diiodomethane	41.6	3.5	41.6	6.1	42.2	3.0	29.6	3.8
Ethylene Glycol	52.9	5.5	—	—	62.6	2.5	27.3	5.1
1-bromonaphthalene	30.7	3.1	32.6	4.7	29.4	2.2	—	—
Tricresylphosphate	—	—	35.8	8.4	—	—	—	—

† From populations of at least 120 separate contact angle determinations.
‡ Triply distilled.

TABLE IX
Calculated mean surface free energies (γ_{SV}) and standard deviations (δ)

Surface	γ_{SV} (mJm^{-2})	δ	γ^p_{SV} (mJm^{-2})	δ	γ^d_{SV} (mJm^{-2})	δ	$\gamma^p_{SV}/\gamma^d_{SV}$ (mJm^{-2})
EA1	38.8	4.0	6.9	6.1	32.0	9.4	0.22
EA2	36.7	3.0	1.9	1.0	34.8	3.9	0.05
Uniprime 3043	37.9	4.5	7.2	9.4	30.7	13.3	0.23
1020 Steel	56.5	7.9	33.7	20.5	22.7	14.0	1.48
Fe_2O_3†	1357	—	1250	—	107	—	11.7

† Reference 2, theoretical calculation.

TABLE X
Parameters for Griffith/Kaelble stability analysis

Surface	R_0	R_{air} (mJm^{-2})	R_{H_2O}	
EA1	1.66	6.71	2.97	(on 1020 steel)
EA2	0.067	6.20	4.59	(on Uniprime 3043)
	2.28	5.33	3.60	(on 1020 steel)
	0.67	6.05	5.21	(on Uniprime 3043)

Downloaded At: 15:38 22 January 2011

distributed in the two cases. A stress analysis of ELPO-primed steel lap shear joints is given in a companion paper.[6] This section deals with the other aspect of bonds to primed joints, which distinguishes them from bonds to cleaned steel; namely the increases in durability as assessed in accelerated environmental tests. As is shown below, these differences are due to differences in the thermodynamic stability of the two types of bonds.

Surface energy determinations using the methods outlined in the Appendix yielded the data compiled in Tables VIII–XII. From Table XI we note that the Uniprime 3043 and EA1 surfaces were of comparable polarity (as evidenced by their polar to dispersion surface energy ratios, but that EA2 was considerably less polar than these two surfaces.* Yet the total mean surface free energy (γ_{SV}) was roughly the same for all three surfaces. These "low" energy surfaces should be contrasted with the degreased 1020 steel and (theoretical) Fe_2O_3 surfaces, whose energies were also given in

* The increased polarity of EA1 compared to EA2 is very likely due to preferential accumulation of polar curing agent at the surface.

TABLE XI
Ratio of critical stress for interfacial failure in H_2O and air environments

System	$\sigma_c(H_2O)/\sigma_c(air)$ (theoretical)	[Avg. shear strength (water immersion)/avg. shear strength (control)] (average of oven and induction cures)
EA1/1020 Steel	0.38	0.0 (premature failure, interfacial)
EA2/1020 Steel	0.46	0.93 (interfacial failure)
EA1/Uniprime 3043	0.74	0.54 (ELPO degradation, mixed failure mode)
EA2/Uniprime 3043	0.86	0.96 (mixed ELPO/phosphate, ELPO/adhesive failure)

Table IX. "High" energy surfaces are dominated by polar forces, while dispersion forces predominate for the lower energy adhesives and the ELPO primer. Thus we would anticipate that an interface between two quite different surfaces, *e.g.*, EA2 and the degreased 1020 steel (or Fe_2O_3) would have a much higher interfacial energy than an interface between EA2 and Uniprime 3043. Consequently, the EA2/3043 interface would be more stable. To quantify this in terms of the Griffith/Kaelble failure criterion,[7] we note from Eq. (11) in the Appendix that the critical stress for interfacial crack propagation is maximized by making the surface-energy-dependent quantity $(R^2 - R_0^2)^{1/2}$ as large as possible. The critical stress can be maximized by decreasing R_0, *i.e.*, by matching polar and dispersive components of the surface free energies of adhesive and substrate.

TABLE XII
Work of adhesion in inert medium (W_A) and work of adhesion in H_2O environment (W_{AL})

Phase 1 (Adhesive)	Phase 2 (Substrate)	W_A (mJm^{-2})	W_{AL} (mJm^{-2})	$W_A - W_{AL}$ (mJm^{-2})
EA1	Fe_2O_3†	303.0	−241.0	544.0
EA1	Degreased 1020 steel	84.4	11.6	72.8
EA1	Uniprime 3043	76.8	40.9	35.9
EA2	Fe_2O_3	219.0	−309.0	528.0
EA2	Degreased 1020 steel	72.1	14.8	57.3
EA2	Uniprime 3043	72.6	52.3	20.3
Uniprime 3043	Fe_2O_3	304.0	−239.0	543.0
Uniprime 3043	Degreased 1020 steel	84.0	11.4	62.6

† Using theoretical values given in Table 9.

Downloaded At: 15:38 22 January 2011

(This is equivalent to lowering the interfacial free energy.) At the same time, R must either stay the same or increase. Increase in R result when the polar and dispersive character of the two mated surfaces are as different as possible from those of the environment.

For EA1 Table X shows that R_0 decreases from 1.66 $(mJm^{-2})^{1/2}$ on degreased 1020 steel to 0.067 $(mJm^{-2})^{1/2}$ on Uniprime 3043. The corresponding values for EA2 are 2.28 $(mJm^{-2})^{1/2}$ on the degreased steel to 0.67 $(mJm^{-2})^{1/2}$ on Uniprime 3043. In a moist environment, R_{H_2O} increases for EA1 and EA2 on changing from the steel to the Uniprime 3043 bonding substrate. Therefore, the change in surface energies is such that $(R^2 - R_0^2)^{1/2}$ is larger for primed substrates, than for the steel. The primer/adhesive interface should, therefore, be more stable in a moist environment than the degreased 1020 steel (or Fe_2O_3)/adhesive interface.

The ratio of critical stress for interfacial crack propagation in a moist environment to that in air for EA1 and EA2 on steel and on Uniprime 3043 are given in Table XI. Also given in Table XI, for purposes of comparison, are ratios of mean lap shear strengths after water immersion, to mean lap shear strengths of controls. According to the calculated critical stress ratios, EA1 and EA2 should show increased durability on Uniprime 3043 substrates compared to steel. However, as noted above, due to primer degradation, EA1 loses considerable strength in a water soak (as well as salt spray) environment. Except where degradation occurred (thus invalidating the thermodynamic analysis) and no comparison could be made, the values of the critical stress ratios correlate with ratios of the mean lap shear strengths. However, recalling the *magnitude* of the lap shear strengths involved (Table III), EA2 is by far the strongest and most durable adhesive. Finally, on the basis of the calculated critical stress ratios (0.46—EA2/steel, 0.86—EA2/Uniprime 3043), EA2 should be more stable in a moist environment when bonded to the primer, than when bonded to steel. However, for this particular accelerated test, there is only a marginal (~3%) increase in strength retention for the EA2/Uniprime 3043 system over the EA2/steel system.

Driving force for water diffusion to adhesive substrate interface

Table XII contains calculated values for W_A, the work required to create unit area of substrate interface by removing adhesive in

Downloaded At: 15:38 22 January 2011

vacuum (or inert atmosphere); and values for W_{AL}, the comparable work in the presence of water. In all cases considered $W_A > W_{AL}$, which indicates the expected instability in the H_2O environment. In addition, the fact that $W_A > W_{AL}$ means that there is a thermodynamic driving force (lowering of free energy) associated with the replacement of adhesive/substrate interface by H_2O saturated adhesive and substrate surfaces.[10]

From Table XII by far the largest calculated variations for W_A and W_{AL} occur in systems involving the very high energy ferric oxide surface. Here $\Delta W = W_A - W_{AL}$ is of the order of 500 mJm^{-2} in all cases, in line with literature values.[2] Next in magnitude are systems where bonds are formed with a degreased 1020 steel surface, and lowest of all are the EA1 and EA2/Uniprime 3043 interfaces. In fact, according to the data in Table XII, EA2 on Uniprime 3043 has a driving force for moisture penetration of the adhesive bond which is 44% smaller than EA1 on Uniprime 3043. It could still be argued that in these systems stability is ultimately determined by the stability of the ELPO/zinc phosphate region, which is highly resistant to corrosion (hence to stress corrosion cracking) in a moist environment. Nonetheless, by reducing the adhesive/substrate interfacial energy, we have in effect removed a weak link in the system, replacing it with a more stable, moisture resistant bond.

Downloaded At: 15:38 22 January 2011

CONCLUDING REMARKS

Although electrodeposited organic primers are in general susceptible to degradation by adhesives during cure, with consequently poor bond strengths and durability, we have shown that for bonded joints where this degradation can be avoided, significant increases in strength and durability can be obtained. Increases in durability were attributed to more favorable energetics for the adhesive/primer and primer/conversion coating interfaces, than for the adhesive/steel interface. As shown in a subsequent study,[6] the increases in strength were attributed to fundamentally different stress distributions for adhesive/primer/steel compared to adhesive/steel joints.

References

1. J. Comyn, in *Developments in Adhesives-2* (Applied Science Publishers, London, 1982), p. 279.
2. R. A. Gledhill and A. J. Kinloch, *J. Adhesion* **6,** 315 (1974).
3. A. J. Kinloch and S. J. Shaw, in *Developments in Adhesives-2* (Applied Science Publishers, London, 1982), p. 83.
4. R. T. Foister, *J. Colloid Interf. Sci.* **116** (1), 109 (1987).
5. P. E. Pierce, *J. Coatings Technology* **53,** 52 (1981).
6. D. W. Schmusser, N. Johnson, and R. T. Foister, "Stress Analysis of Adhesively Bonded, Electroprimed Steel Lap Shear Joints," J. Adhesion (in press).
7. D. H. Kaelble, *J. Applied Polym. Sci.* **18,** 1869 (1974).
8. R. W. Adamson, *Physical Chemistry of Surfaces* (4th Edition) (John Wiley & Sons, New York, 1982), p. 340.
9. W. D. Harkins, *Physical Chemistry of Surface Films* (Reinhold, New York, 1952), p. 199.
10. D. H. Kaelble, *Physical Chemistry of Adhesion* (Wiley-Interscience, New York, 1971).
11. C. A. Ward, A. W. Neumann, *J. Colloid Interf. Sci.* **49,** (2), 286 (1974).
12. D. H. Kaelble, P. J. Dynes, L. Maus, *J. Adhesion* **6,** 239 (1974).
13. G. E. Hammer, L. T. Drzal, *Appl. Surf. Sci.* **4,** 340 (1980).
14. A. A. Griffith, *Phil. Trans. Roy. Soc. (London)* **A221,** 163 (1921).
15. R. T. Foister and R. K. Gray, U.S. Patent 4,544,432, October 1, 1985.
16. R. T. Foister, *J. Colloid Interf. Sci.* **96** (1), 386 (1983).
17. R. T. Foister, *ibid.,* **99** (2), 568 (1984).

Downloaded At: 15:38 22 January 2011

APPENDIX

PROCEDURES FOR DETERMINING SURFACE, INTERFACIAL ENERGIES AND BOND STABILITY

Surface energies via contact angle measurement

Young's equation for the mechanical/thermal equilibrium of a liquid drop on a smooth solid surface is given by[8]

$$\gamma_{SV} - \gamma_{SL} = \gamma_{LV} \cos \theta_e, \tag{1}$$

where

γ_{SV} = Solid free energy per unit surface area
γ_{SL} = Solid/liquid free energy per unit interfacial area
γ_{LV} = Liquid surface tension

and θ_e is the equilibrium contact angle that the liquid meniscus makes with the solid surface.

The work required to create a unit area of solid *in vacuum,* the

work of adhesion W_A, where[8]

$$W_A = \gamma_S + \gamma_{LV} - \gamma_{SL}. \tag{2}$$

Here γ_S is the surface free energy of the solid in vacuum. Finally, the lowering of solid surface free energy by adsorption of liquid vapor is given by the equilibrium "spreading pressure" Π_e,

$$\Pi_e = \gamma_S - \gamma_{SV}. \tag{3}$$

Thus, combining Eqs. (1)–(3) we may write a "nominal"[7] work of adhesion W'_A as

$$W'_A = W_A - \Pi_e = \gamma_{LV}(\cos\theta_e + 1). \tag{4}$$

By analogy with the definition of W_A, it is seen that

$$W'_A = \gamma_{SV} + \gamma_{LV} - \gamma_{SL} \tag{5}$$

is the work of adhesion required to create a unit area of solid in equilibrium with liquid vapor, starting with contact of the liquid with the solid. The term "nominal" work of adhesion refers to the fact that W_A and Π_e are often of equal magnitude.[9]

To obtain a measure of the solid surface energy γ_{SV} it is assumed[10] that each of the three energies can be expressed as a sum of polar (p) and dispersion (d) contributions:

$$\gamma_{SV} = \gamma^p_{SV} + \gamma^d_{SV},$$
$$\gamma_{LV} = \gamma^p_{LV} + \gamma^d_{LV},$$

and

$$\gamma_{SL} = \gamma^p_{SL} + \gamma^d_{SL}. \tag{6}$$

Thus, applying the "geometric mean" approximation[10] to the interfacial free energy γ_{SL} in Eq. (5),

$$W'_A = [(\gamma^d_{SV}\gamma^d_{LV})^{1/2} + (\gamma^p_{SV}\gamma^p_{LV})^{1/2}]. \tag{7}$$

For two liquids (i, j) with known polar (γ^p_{LV}) and dispersion (γ^d_{LV}) components of surface tension, Kaelble[10] writes two equations which may be solved for the two unknowns γ^p_{SV} and γ^d_{SV}:

$$1 + \cos\theta_{e(i)} = \frac{2}{\gamma^{(i)}_{LV}}[(\gamma^p_{SV}\gamma^p_{LV(i)})^{1/2} + (\gamma^d_{SV}\gamma^d_{LV(i)})^{1/2}] \tag{8}$$

$$1 + \cos\theta_{e(j)} = \frac{2}{\gamma^{(j)}_{LV}}[(\gamma^p_{SV}\gamma^p_{LV(j)})^{1/2} + (\gamma^d_{SV}\gamma^d_{LV(j)})^{1/2}] \tag{9}$$

Downloaded At: 15:38 22 January 2011

It is important to emphasize that *by definition* γ_{SV} is not a property of the solid surface alone. It is in general a measure of solid/vapor equilibrium. However, for low surface energy organic solids, such as adhesives, the spreading pressure Π_e is approximately equal to zero,[11] consequently $\gamma_S \cong \gamma_{SV}$. Thus $W_A \approx W'_A$ (see Eq. (4)) and γ_{SV} determined in the manner outlined above should be roughly equal to γ_S. For higher energy surfaces, however, $\Pi_e \neq 0$, and may in fact be quite high.[9] Measurements of γ_{SV} for metallic oxides are, therefore, of dubious thermodynamic significance, although a number of authors have argued that W'_A should correlate with adhesive tests where metal/adhesive bonds are made and broken under ambient conditions.[7,12,13]

For EA1, EA2, and Uniprime 3043 surfaces, we expect that, for the liquids used in these studies (see Table I), $\Pi_e \cong 0$. Recognizing the difficulties with high energy surfaces discussed above, we have measured γ_{SV} for the degreased 1020 steel surface by the same method, but we use this number merely as a baseline for comparing the steel/adhesive and ELPO/adhesive interfaces. Theoretical values of γ_S^p and γ_S^d are available[2] for pure Fe_2O_3 (ferric oxide) surfaces, and we have also used these values in certain calculations below. Thus where "degreased 1020 steel" is denoted, γ_{SV}^p and γ_{SV}^d values are used. For a surface denoted "ferric oxide," we have used the literature values for γ_S^p and γ_S^d.

Downloaded At: 15:38 22 January 2011

Bond stability analysis

By combining the surface energy analysis above with Griffith's[14] failure criterion for elastic crack propagation, Kaelble[7] has shown that

$$\sigma_c \text{ (critical stress for interfacial crack propagation)} \sim (R^2 - R_0^2)^{1/2}, \tag{10}$$

where

$$R^2 = [(\alpha_2 - H)^2 + (\beta_2 - K)^2] \tag{11}$$

$$R_0^2 = \tfrac{1}{4}[(\alpha_1 - \alpha_3)^2 + (\beta_1 - \beta_3)^2] \tag{12}$$

$$H = \tfrac{1}{2}(\alpha_1 + \alpha_3) \tag{13}$$

$$K = \tfrac{1}{2}(\beta_1 + \beta_3) \tag{14}$$

$$\alpha = (\gamma_{SV}^{d})^{1/2} \tag{15}$$

$$\beta = (\gamma_{SV}^{p})^{1/2}. \tag{16}$$

For example, the ratio of σ_c in water to σ_c in air is a measure of the relative stress required to obtain interfacial failure ("adhesive" failure) in the two environments.

Thermodynamic driving force for moisture diffusion

We have mentioned above that the energy required to separate a metal/adhesive bond decreases as the bond ages in a moist environment. In terms of the work of adhesion, it has been shown[2] that this statement is equivalent to the inequality

$$W_A > W_{AL}, \tag{17}$$

where W_A is the work of adhesion required to create a unit area of solid surface by adhesional failure in vacuum (the solid/solid analogue of Eq. (2), which is for a solid/liquid system). Likewise W_{AL} is the work of adhesion required to create a unit area of the same solid surface by adhesional failure, but this time in the presence of a wetting liquid L (water). Measurements for epoxy adhesives bonded to ferric oxide[2] show that $W_A > 0$ and that $W_{AL} < 0$. Remembering the relation between work and free energy, it is apparent that the free energy change, for moisture penetration followed by bond failure, is negative. This decrease in free energy represents a thermodynamic driving force for water transport to the adhesive/substrate interface.

Downloaded At: 15:38 22 January 2011